J. Min. Metall. Sect. B-Metall. 54 (2) B (2018) 251 - 260

Journal of Mining and Metallurgy, Section B: Metallurgy

WETTING AND INTERFACIAL REACTIONS: EXPERIMENTAL STUDY OF THE Sb-Sn-X (X = Cu, Ni) SYSTEMS

R.M. Novaković [a*], S. Delsante [a,b], G. Borzone [a,b]

[a] Institute of Condensed Matter Chemistry and Energy Technologies-National Research Council (ICMATE-CNR), Genoa, Italy

[b] Department of Chemistry and Industrial Chemistry, Genoa University and Genoa Research Unit of the National Consortium of Materials Science and Technology (INSTM), Genoa, Italy

(Received 24 January 2018; accepted 29 June 2018)

Abstract

Experimental studies of the Cu-Sb-Sn and Ni-Sb-Sn systems have been carried out by the wetting tests, followed by the analysis of the microstructural evolution occurring at the interface between the liquid alloy and solid substrate. The wetting experiments on the $Sb_{30}Sn_{70}$ / (Cu, Ni) and $Sb_{38.4}Sn_{61.6}$ / (Cu, Ni) systems have been performed by using a sessile drop apparatus. The wetting behaviour of the two alloys in contact with Cu-substrate differs from that observed in the case of Ni-substrate. The Sb-Sn alloy / substrate interface was characterised by SEM-EDS analyses. For each system, the solid-liquid interactions and the phases formed at the interface were studied with the help of the corresponding phase diagrams.

Keywords: *Wetting experiments; Sb-Sn Alloys; Cu-and Ni-substrates; Interfaces; CALPHAD*

1. Introduction

Sb-Sn alloys containing up to 15 at % Sn are used as high temperature lead free solders [1-4] in the step soldering process, which requires the formation of consecutive joints [5]. Similarly, various Sb-Sn-based multicomponent alloys with melting temperatures higher than 500 K have been investigated and among them, Ag-Sb-Sn [6], Cu-Sb-Sn [2], Sb-Sn-Zn [7] and Ag-Cu-Sb-Sn [8-10] solders are already used for advanced packing technologies [4,5].

The COST Action MP0602 "Advanced Solder Materials for High Temperature Application" (HISOLD) has been dedicated to the investigation and design of high temperature lead free solders and the results obtained are reported in [11-13]. Another important application of Sb-Sn alloys and/or Sb-Sn based composites is related to their use as anodic materials for Li-batteries. Indeed, high Li-storage capacity and good cycling stability of Sb-Sn alloy powders make them suitable for rechargeable Li-batteries [14-17]. Among Sb-Sn alloy compositions, it seems that the use of SbSn intermediate phase at the equiatomic composition is beneficial during lithiation due to its separation into the more lithiated and/or not lithiated phases helping to relieve mechanical strain [15]. Although the investigation of the Sb-Sn system started more than one hundred years ago [18], until nowadays at least twenty assessments of its phase diagram are available [19-32], and even after recent experimental studies [31,32] some questions concerning the existence of a Sb_3Sn_4-SbSn two-phase field and of ordering phenomena in the SbSn phase are still open.

Thanks to long lasting experience related to the investigation of lead-free solders by wetting experiments [1,8,33,35], we can state that the microstructure evolution after wetting tests is qualitatively comparable to that of a real solder joint [36,37]. Therefore, the interfacial reactions between liquid alloys and solid substrates and the phases subsequently formed at the interface, identified by SEM-EDS analyses, can be analysed by means of the corresponding phase diagrams. On the other hand, lacking direct thermodynamic measurements as in the case of high melting temperature systems, the data describing the solid-liquid interface formed during the wetting tests can be used as the input to calculate the phase equilibria [38]. The wetting behaviour of any liquid in contact with a solid surface is expressed by the contact angle Θ that the liquid drop forms on the solid substrate. Another important parameter is the work of adhesion W_A that depends on the bonding characteristics of both, the liquid and the solid phase as well as on the interactive forces at their interface formed during wetting tests [39]. As already mentioned above, there are lot of literature data describing the wetting of Sn-rich alloys in contact

*Corresponding author:rada.novakovic@ge.icmate.cnr.it

DOI:10.2298/JMMB180124013N

CC BY SA

with Cu-substrate and only a few datasets for Ni-substrate [1]. On the contrary, concerning intermediate alloy compositions, the wetting behaviour of the Sb-Sn / (Cu, Ni) systems has not yet been investigated.

In the present work, the $Sb_{30}Sn_{70}$ and $Sb_{38.4}Sn_{61.6}$ (at %) alloys on Cu and Ni-substrates were used for wetting experiments that were carried out by the sessile drop method. Subsequently, SEM-EDS analyses were done and the results obtained were analysed in terms of the Sb-Sn-X (X = Cu, Ni) phase diagrams.

2. Experimental

2.1. Materials

The $Sb_{30}Sn_{70}$ and $Sb_{38.4}Sn_{61.6}$ (in at %) alloys were prepared from pure Sn bar (Newmet Koch, 99.9999 wt %) and Sb ingots (Newmet Koch, 99.999 wt %). After mechanical cleaning proper amounts of Sb and Sn were weighted with accuracy of ± 0.05 mg, encapsulated inside a quartz tube, sealed under Argon atmosphere, and induction melted for three times. The homogenization was achieved by shaking at different speeds. Subsequently the $Sb_{30}Sn_{70}$ and $Sb_{38.4}Sn_{61.6}$ alloys were water quenched. All ingots were checked by SEM-EDS analyses to ensure proper composition and uniform structure and subsequently were cut into small samples of around 1 g.

2.2. Wetting tests

The sessile drop method has been applied to evaluate the wetting behaviour of the $Sb_{30}Sn_{70}$ and $Sb_{38.4}Sn_{61.6}$ alloys on Cu and Ni-substrates. A standardized experimental procedure has been described in detail for other alloys of the same system [1].

The contact angles were measured using $Sb_{30}Sn_{70}$ and $Sb_{38.4}Sn_{61.6}$ alloy samples, previously mechanically cleaned by scratching, chemically rinsed with pure ethanol in an ultrasonic bath, introduced at the centre of the chamber and placed on Cu or Ni-substrate (both with a purity of 99.9999 %, square plate, 13x13x1 mm). To reach a surface roughness of $R_a \sim 0.05\ \mu m$, Cu and Ni-substrates were previously metallographically mirror polished. Before the test, the furnace was heated and degassed under vacuum ($P = 10^{-4}$ Pa), then pure Argon (ArN60) was introduced. The resulting oxygen pressure was around an average value of $p_{o2} \leq 10^{-6}$ Pa. The isothermal measurements were carried out at different temperatures over the interval T_{liq} + 50 K- 900 K (is the liquidus temperature). During experiments, the temperature was measured by a K-type thermocouple and kept constant within ± 2 K and the drop profile was acquired by a CCD camera with a precision of ± 1μm. The image was processed in LABview environment using home-made A.S.T.R.A.view® software [40] and the contact angle data were evaluated with an accuracy of ± 0.5°. The left and right contact angle values differ less than 3 % and the contact angle data given in Table 1 represent an average value of the two values.

After wetting experiments, the drop / substrate couples were cooled down to room temperature and the interfacial microstructure of each solidified sample was characterized by optical microscopy and SEM-EDS analyses on the cross-section mirror polished.

3. Results and discussion

Until now, only Sn-rich alloys containing up to 15 at % of Sb have been studied aiming to develop a series of new high temperature lead-free solders. Indeed, the wetting behaviour of a liquid Sb-Sn / solid Cu system has been studied in [1,2,4,41-42], while in the case of Ni-substrate only two datasets were reported [1]. The aim of the present research is twofold: to determine the wetting behaviour of abovementioned systems and to substantiate the phase equilibria determination in the Cu-Sb-Sn and Ni-Sb-Sn ternary systems. Therefore, the wetting properties of the $Sb_{30}Sn_{70}$ / (Cu, Ni) and $Sb_{38.4}Sn_{61.6}$ / (Cu, Ni) systems were determined and the test parameters such as the initial (T_0) and the final (T_f) temperatures of the experiments together with the corresponding contact angles (Θ_0) and (Θ_f) respectively, and the duration of the experiments conducted under isothermal conditions (t_f) are given in Table 1. The liquidus temperatures (T_{liq}) of the alloys studied refer to the Sb-Sn phase diagram [31].

The microstructural characterisation of the Sb-Sn/(Cu, Ni) systems investigated has been done by SEM-EDS and the results obtained were analysed in view of the corresponding binary and ternary phase diagrams. The reaction layers formed at the interface between liquid $Sb_{30}Sn_{70}$ and $Sb_{38.4}Sn_{61.6}$ alloys in contact with the two substrates have irregular morphology. In the case of Cu-substrate, a characteristic so-called “scallop” morphology is

Table 1. *Wetting properties of liquid Sb-Sn alloys in contact with Cu and Ni-substrates and test parameters*

Alloy composition / at %	Temperature / K			Substrate				Time / min
				Cu		*Ni*		
	T_{liq}	T_0	T_f	$\theta_0(^o)$	$\theta_f(^o)$	$\theta_0(^o)$	$\theta_f(^o)$	t_f
$Sb_{30}Sn_{70}$	624	640	795	130	43	-	-	60
$Sb_{38.4}Sn_{61.6}$	665	695	785	126	29	-	-	38
$Sb_{30}Sn_{70}$	624	650	790	-	-	127	37	56
$Sb_{38.4}Sn_{61.6}$	665	663	672	-	-	143	46	10

CC BY SA

particularly pronounced as it was already observed for various Sn-rich solders [1,8,43,44]. The estimation of layer thickness by means of SEM-EDS analyses is related to some errors even if the variations of thickness are very small. Higher uncertainties are introduced to estimate the thickness of interfacial layer with completely irregular morphology such as that of the scallop type. The thickness of each layer (Table 2) represents a mean value calculated from real thickness values measured in different points along a cross section, as it was reported in previous works [1,8].

3.1. Wetting behaviour of Sn-Sb / Cu systems

The contact angle values of 43 and 29° were determined for liquid $Sb_{30}Sn_{70}$ and $Sb_{38.4}Sn_{61.6}$ alloys respectively, in contact with solid copper (Table 1), indicating a good wettability of Cu-substrates. Neither there are available data on the wetting properties for the alloys investigated here nor for the alloys with similar compositions and therefore the results obtained cannot be compared, but the effect of Sb on their wetting behaviour can be analysed. For the experimental conditions applied, the contact angle values of the two alloy compositions indicate that higher Sb-content in the alloy results in an improvement in wetting. The same was deduced for Sb-Sn solders tested under similar conditions [1]. On the contrary, under different experimental conditions, some wetting tests performed on Sb-Sn solders showed that an increase in Sn promotes the wetting on Cu-substrate [2]. Sb-Sn melts wet and react with Cu-substrate arriving at low contact angles, but with significant modification of the initial metal-metal interface. The wetting was observed after alloy melting, and it was mainly driven by the high dissolutive reactivity of the Sb-Sn/Cu system and subsequent formation of a scallop type interface [1].

Interfacial reactions and the phases formed at the interface of the $Sb_{30}Sn_{70}$ / Cu and $Sb_{38.4}Sn_{61.6}$ / Cu systems are similar to those observed for Sn-rich alloys on Cu-substrates [1,8]. In both cases, Sn/Cu couples can simply describe the main reaction products [44] that are defined by the Cu-Sn phase diagram [26,45]. Indeed, the Cu-Sn system is characterised by the presence of the two energetically favoured phases, i.e. ε-Cu_3Sn and η-Cu_6Sn_5 with narrow solubility ranges, i.e. $23.5 \leq Sn\ (at\ \%) \leq 27.1$ and $43.5 \leq Sn\ (at\ \%) \leq 45.5$, respectively. Usually the ε-Cu_3Sn phase was experimentally found adjacent to Cu-substrate, while the η-Cu_6Sn_5 was adjacent to the solder [1,8,33,34,44]. Comparing the two phases η-Cu_6Sn_5 results more stable [46]. The experimental values of the growth-rate coefficients at T = 453 K are $k^{\varepsilon} = 4.40 \cdot 10^{-9}$ and $k^{\eta} = 7.76 \cdot 10^{-9}$ $m \cdot s^{-0.5}$ [47] and the growth of the two phases is diffusion controlled obeying the parabolic law [48]. Based on it, an increase in reaction time leads to a more pronounced growth of η-Cu_6Sn_5 with respect to that of ε-Cu_3Sn [44,49]. The solid-liquid interaction phenomena observed during the wetting tests and the phases formed at the interface identified by SEM-EDS analyses can be interpreted in terms of the phase equilibria, taking into account the recent assessment of the Cu-Sb-Sn phase diagram [50-52]. The phase equilibria in the Cu-Sb-Sn system were studied by [50], using the samples equilibrated for long times, i.e. Sn-rich alloys were annealed for about 2 months at T = 523 K. Differential scanning calorimetry (DSC) and Electron Probe Micro Analyses (EPMA) were employed to study the Cu-Sn-Sb system along the Sn:Sb=1:1 isopleth and to identify five invariant ternary reactions [51,52]. Among the primary solidification phases in the Cu-Sb-Sn liquidus projections, the ε-Cu_3Sn, η-Cu_6Sn_5, (Sn), Sb_2Sn_3, SbSn, Sb_4Sn_3 and (ε-Cu_3Sb, Cu_4Sn) were also detected at the interfaces of the Sb-Sn/Cu systems investigated by the wetting tests. The present results

Table 2. *SEM-EDS characterisation of the Sb-Sn / (Cu; Ni) interfacial microstructure*

Nominal alloy composition (at %) and substrate	Interface composition (at %)	Layer Thick-ness (μm)	Time min	T_f (K)	Bulk-phase composition (at %)
$Sb_{30}Sn_{70}$ / Cu	Cu–2.4Sb–24.4Sn (ε - Cu_3Sn)* Cu–14.4Sb–34.4Sn (η - Cu_6Sn_5)*	30 18	60	795	Sb–55.7Sn (SbSn-phase)
$Sb_{38.4}Sn_{61.6}$ / Cu	Cu–5.5Sb–21.2Sn (ε - Cu_3Sn)* Cu–19.4Sb–30.8Sn (η - Cu_6Sn_5)*	25 20	38	785	Sb–50.2Sn (SbSn-phase)
Sb30Sn70 / Ni	Ni–18.2Sb–9.7Sn (Ni_3Sn)* Ni–34.1Sb–19.6Sn (ζ near the interface)*	< 6 10	56	790	Sb–56.0Sn (SbSn-phase)
$Sb_{38.4}Sn_{61.6}$ / Ni	Ni–46.0Sb –31.7Sn (τ)* Ni–48.0Sb –29.5Sn (τ near the interface)*	< 4 7	10	672	Sb–55.8Sn (SbSn-phase)

* *The phase detected is based on that indicated in the bracket*

CC BY SA

suggest that an increase in Sb-content leads to a decrease in the thickness of the interface layer formed between the Sb-Sn alloy and Cu-substrate (Table 2), indicating that Sb is not actively involved in the interfacial reactions, as it was already observed [1,53]. The solubility of Sb in Cu_6Sn_5 phase up to 6.5 reported in [54] differs significantly from that of 11 (both in at %) obtained from the equilibria studies of the Cu-Sb-Sn system at T=533 K [50]. After the last isothermal steps of wetting tests (Table 2), the interfacial reactions of liquid $Sb_{30}Sn_{70}$ and $Sb_{38.4}Sn_{61.6}$ alloys in contact with Cu-substrate for temperatures varying between 785 and 795 K were investigated. Until now, no available experimental data on the Cu-Sb-Sn phases formed at these temperatures.

3.1.1. $Sb_{30}Sn_{70}$ / Cu

The contact angle variations have been determined under isothermal conditions at four temperatures (640, 690, 745, 795 K) and for times of about 10 ± 2 min at each temperature (Fig. 1). During heating up to T = 640 ± 1 K, at the beginning of the first isothermal cycle, the contact angle value drop down from Θ = 130° to Θ = 48°, observed, after 12 min. A further decrease in the contact angle values, i.e. from Θ = 48° to Θ_f = 43° was observed at T = 795 K after 60 min, when the last isothermal cycle was completed (Fig. 1; Table 1).

The solidified $Sb_{30}Sn_{70}$ / Cu sample was metallographically prepared and the cross section was characterised by SEM-EDS analyses. As in the case of Sb-Sn solders [1], Cu-solubility in the liquid alloy and subsequent dissolution of Cu-substrate determine the interfacial microstructure of the $Sb_{30}Sn_{70}$ / Cu system. Significant dissolution occurs over the whole interface area and the formation of the crater with a maximum depth of about 40 µm under the drop was observed (Fig. 2a). Because of this, the final value of the contact angle, Θ_f = 43° can be considered as an "apparent" contact angle [55].

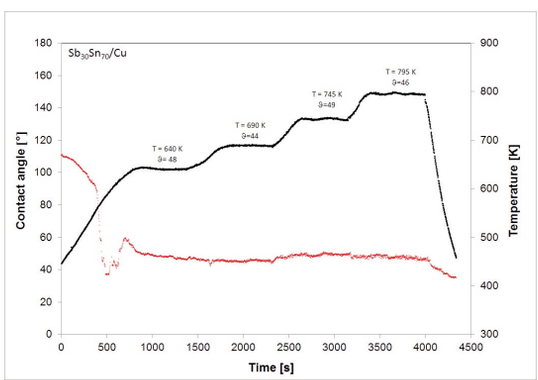

***Figure 1**. Contact angle (◆) and temperature (•) as function of time for the $Sb_{30}Sn_{70}$ alloy on Cu-substrate*

As it is shown in Fig. 2a and Fig. 2b (an enlarged interface area), the formation of two reaction layers was observed. Close to Cu-substrate an interface layer of the Cu-2.4Sb–24.4Sn phase (30 µm) having the composition close to ε-Cu_3Sn was detected and adjacent to this layer, the Cu-14.4Sb–47.5Sn phase (18 µm), with composition close to η-Cu_6Sn_5, was identified (Fig. 2b; Table 2). Taking into account that the solubility of Sb in η-Cu_6Sn_5 increases with temperature, the value of 14.4 at % found at T= 795 K (Table 2) might be considered comparable to that of 11 at % determined at T= 533 K [50]. As it was already observed for Sn-rich alloys in contact with Cu-substrates [1,8], the thickness of both scallop type interfacial layers is not uniform. The brightest regions in Fig. 2a and Fig. 2b correspond to the Sb-(56.1 ± 0.4) Sn phases indicating the presence of SbSn solid solutions [31,32].

The analysis of the solidified drop border composition near Cu-substrate (Fig. 2c) indicates the presence of phases based on ε -Cu_3Sn with an average composition of Cu-6.5Sb-19Sn. Due to a strong exothermic reaction that occurs during wetting experiments on Cu-substrate, small areas and spots having the compositions of Cu-(3.5 ± 0.5)Sb-(13.8 ± 2) Sn were found. On the top drop Sb_3Sn_4 based phases having the composition of Cu-(40.5 ± 1.0)Sb-(57.6 ± 1.0) Sn and containing up to 2.2 at % Cu were identified (Fig. 2c). The alloys based on ε -Cu_3Sn and η-Cu_6Sn_5 phases together with the 25.7Sb-74.3Sn are slightly different from the nominal alloy composition, i.e. the Sb-70Sn as well as Sn-rich alloy compositions containing up to 6 at % of Cu were also detected on the top drop (Fig. 2d).

3.1.2. $Sb_{38.4}Sn_{61.6}$ / Cu

The contact angle variations have been determined under isothermal conditions at two temperatures (695, 785 K) and for times of about 10 ± 2 min at each temperature (Fig. 3). During heating up to T = 695 ± 1 K, at the beginning of the first isothermal cycle, the contact angle values drop down from 126 to Θ = 44°, observed after 11 min. The contact angle further decreased from Θ = 44° to Θ = 29°, observed at T = 785 K after 38 min, when the last isothermal cycle was completed (Fig. 3; Table 1).

As in the case of the $Sb_{30}Sn_{70}$ / Cu dissolutive wetting was observed and the formation of a groove with a maximum depth of about 20 µm under the drop (Fig. 4a) indicates that the contact angle of Θ_f = 29° is the "apparent" one (Table 2). The two reaction layers formed at the $Sb_{38.4}Sn_{61.6}$ / Cu interface were detected by SEM-EDS analyses (Fig. 4a and Fig. 4b). Close to Cu-substrate, an interface layer based on ε -Cu_3Sn having the composition of Cu-5.5Sb-21.2Sn (25 µm), and the second layer with the composition of

CC BY SA

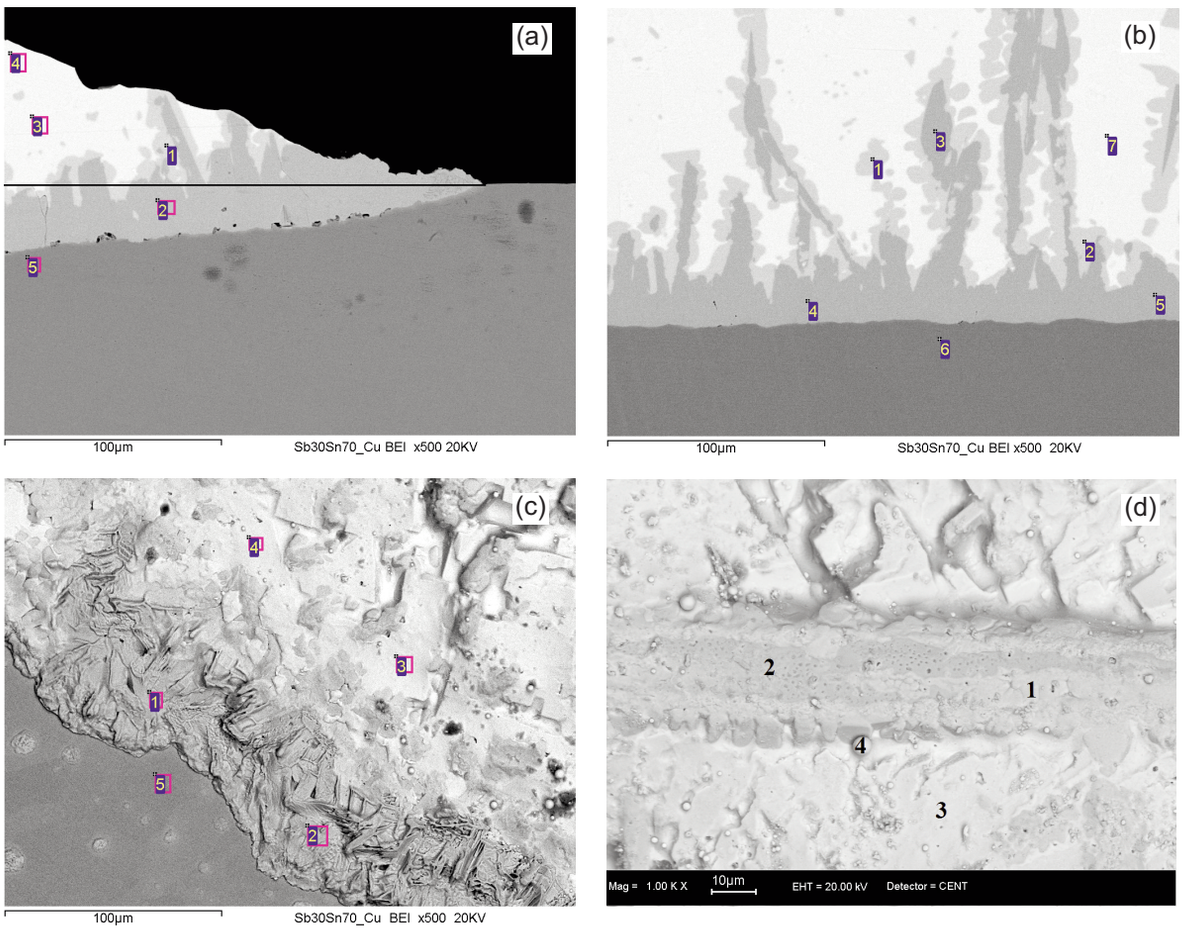

Figure 2. *$Sb_{30}Sn_{70}$ / Cu system. SEM micrograph of a) Cross section of the sessile drop: The formation of two reaction layers at the alloy/substrate interface 1 – Cu-14.4Sb-34.9Sn (η-Cu_6Sn_5 based phase) and 2 – Cu-2.4Sb-24.6Sn (ε-Cu_3Sn based phase); 3 – 43.1Sb-56.9Sn (SbSn phase); 4 –38.1Sb-61.9Sn (close to Sb_2Sn_3 phase); 5 – Cu-substrate. b) Cross section of the solid/liquid interface with reaction layers (Table 2): 1 – Cu-13.3Sb-37.2Sn and 2 – Cu-14.4Sb-34.4Sn (η-Cu_6Sn_5 based phase); 3 – Cu-3.0Sb-25.0Sn, 4 – Cu-2.9Sb-24.4Sn and 5 – Cu-3.0Sb-24.7Sn (ε-Cu_3Sn based phase); 6 – Cu-substrate; 7 – 44.3Sb-55.7Sn (SbSn phase). c) Solidified drop border close to Cu-substrate: 1 – Cu-6.9Sb-18.5Sn and 2 – Cu-6.0Sb-19.6Sn (ε-Cu_3Sn based phase); 3 – Cu-41.5Sb-56.8Sn (Sb_3Sn_4 based phase); 4 – Cu-39.3Sb-58.6Sn (Sb_3Sn_4 based phase); 5 – Cu-substrate. d) Top drop: 1 – Cu-11.5Sb-36.1Sn (η-Cu_6Sn_5 based phase); 2 – Cu-4.5Sb-25.8Sn (ε-Cu_3Sn based phase); 3 – 25.7Sb-74.3Sn and 4 – Cu-6.0Sb-88.1Sn (Sn-rich alloy compositions)*

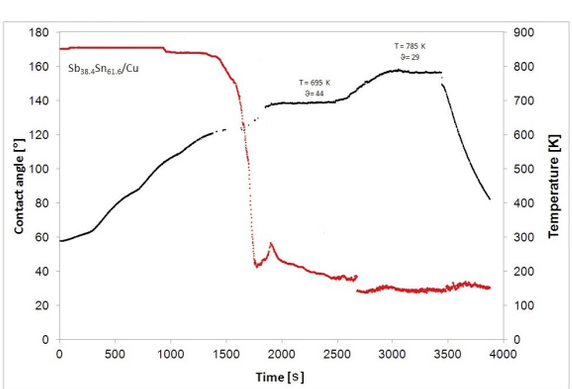

Figure 3. *Contact angle (◆) and temperature (•) as function of time for the $Sb_{38.4}Sn_{61.6}$ alloy on Cu-substrate*

Cu-30.8Sn-19.4Sb (20 μm) were detected (Table 2). The last one is based on η- Cu_6Sn_5, and at T=785 K it has significant Sb-solubility of 19.4 at %, that might be comparable to that of 11 at % observed at T= 533 K by Chen et al. [50]. Both interfacial layers have a non-uniform thickness related to characteristic scallop type morphology (Fig. 4b) described everywhere [1, 8,44]. The brightest regions in Fig. 4a and Fig. 4b correspond to the Sb-(50.4 ± 0.6)Sn phases, identified on the Sb-Sn phase diagram as SbSn solid solutions [31,32].

The analysis of the solidified drop border composition close to Cu-substrate (Fig. 4c) indicates the presence of phases based on η-Cu_6Sn_5, with an average composition of Cu-(19.6 ± 1.3)Sb-(26.1 ± 2.5)Sn. On the top drop Cu-46.3Sb-51.8Sn (SbSn

solid solutions) containing up to 1.9 at % Cu (Fig. 4c), and Sb_3Sn_4 based phase with the composition of 42.1Sb-57.9Sn (Fig. 4d) were identified.

3.2. Wetting behaviour of Sn-Sb / Ni systems

The contact angles of 37 and 46° were determined for liquid $Sb_{30}Sn_{70}$ and $Sb_{38.4}Sn_{61.6}$ alloys respectively, in contact with solid nickel (Table 1), indicating a good wettability of Ni-substrates. The spreading behaviour of the two Sb-Sn alloys investigated is similar to that observed for Sn-rich solder alloys in contact with Ni-substrate [1,8,35] indicating that the contact angle decreases in a stepwise manner with increasing temperature, as observed in [1]. For the alloy compositions investigated, no available literature data for a comparison. Due to some experimental problems, the wetting test on the $Sb_{38.4}Sn_{61.6}$ / Ni was carried out under isothermal conditions at only one temperature, which was about 100 K lower in comparison to other operating temperatures, and for very short time with respect of the other wetting tests given in Table 1. Therefore, the effect of Sb-content on the wetting properties of the systems investigated cannot be deduced.

Significant difference in wetting behaviour of liquid Sb-Sn alloys on Ni- and Cu-substrates is related to a lower dissolution rate of solid Ni [56] controlled by diffusion in the liquid phase in comparison to that of solid Cu [57]. On the other side, the diffusivity data [56,57] indicates that Ni atoms diffuse slower into Sn-rich melts with respect to those of Cu and, in the case of the Sb-Sn/Ni interfaces, the intermetallic compounds with lower thickness were formed

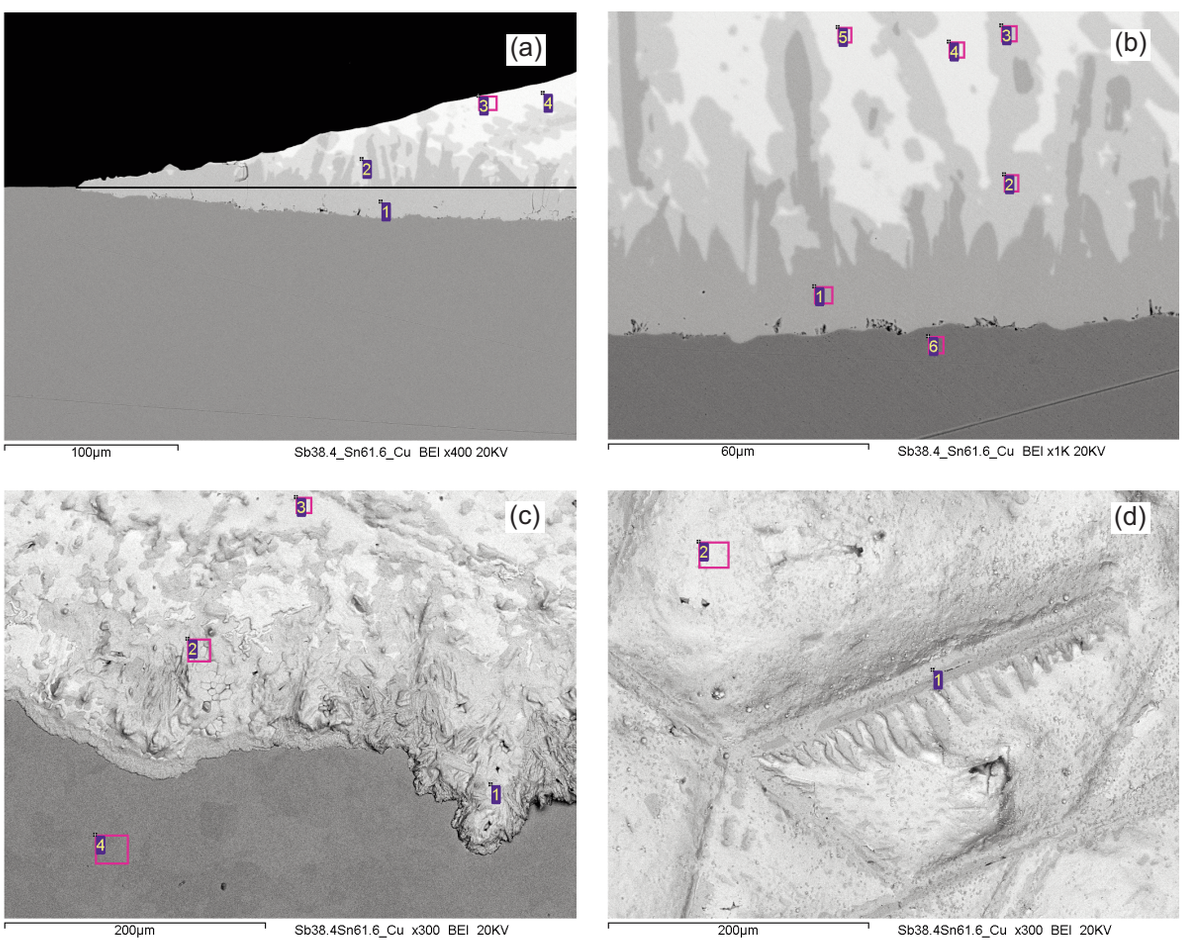

Figure 4. *Sb38.4Sn61.6 / Cu system. SEM micrograph of a) Cross section of the sessile drop: The formation of two reaction layers at the alloy / substrate interface 1 – Cu-5.1Sb-21.8Sn (ε-Cu_3Sn based phase) and 2 – Cu-18.7Sb-30.9Sn (η-Cu_6Sn_5 based phase); 3 – 48.1Sb-51.9Sn and 4 – 45.7Sb-54.3Sn (SbSn phase). b) Cross section of the solid/liquid interface with reaction layers (Table 2): 1 – Cu-5.5Sb-21.2Sn (ε-Cu_3Sn based phase), 2 – Cu-19.5Sb-30.1Sn and 3 – Cu-19.4Sb-30.7Sn (η-Cu_6Sn_5 based phase); 4 – 49.4Sb-50.6Sn and 5 – 49.8Sb-50.2Sn (SbSn phase); 6 – Cu-substrate. c) Solidified drop border close to Cu-substrate: 1 – Cu-20.9Sb-23.6Sn and 2 – Cu-18.4Sb-28.6Sn (η-Cu_6Sn_5 based phase); 3 – Cu-46.3Sb-51.8Sn (SbSn based phase); 4 – Cu-substrate; d) Top drop: 1 – Cu-16.8Sb-30.7Sn (η-Cu_6Sn_5 based phase); 2 – 57.9Sn-42.1Sb (Sb_3Sn_4 based phase)*

CC BY SA

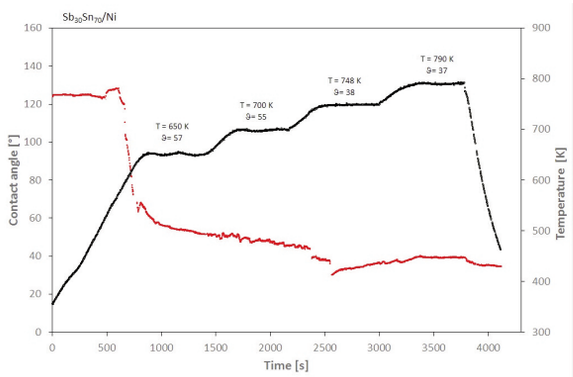

Figure 5. *Contact angle (◆) and temperature (•) as function of time for the $Sb_{30}Sn_{70}$ alloy in Ni-substrate*

[1,8,58]. Similarly, for liquid $Sb_{30}Sn_{70}$ and $Sb_{38.4}Sn_{61.6}$ alloys in contact with Ni-substrates the macroscopically planar interfaces consisting of thin reaction layers were observed (Fig. 6a and Fig. 6b). Sn/Ni couples describe the main reaction products [44,58] and the phases detected by SEM-EDS (Table 2) were analysed in terms of the Ni-Sn [59], Sb-Sn [31,32] and Ni-Sb-Sn phase diagrams [60,61]. The information on the Ni-Sb-Sn system were summarised in [61] and until now they are not yet completed. The present results obtained at temperatures of 790 and 672 K can be helpful to determine the equilibrium phases at the corresponding isothermal sections.

3.2.1. $Sb_{30}Sn_{70}$ / Ni

The contact angle variations have been determined under isothermal conditions at four temperatures (650, 700, 748, 790 K) and for times of about 10 ± 1

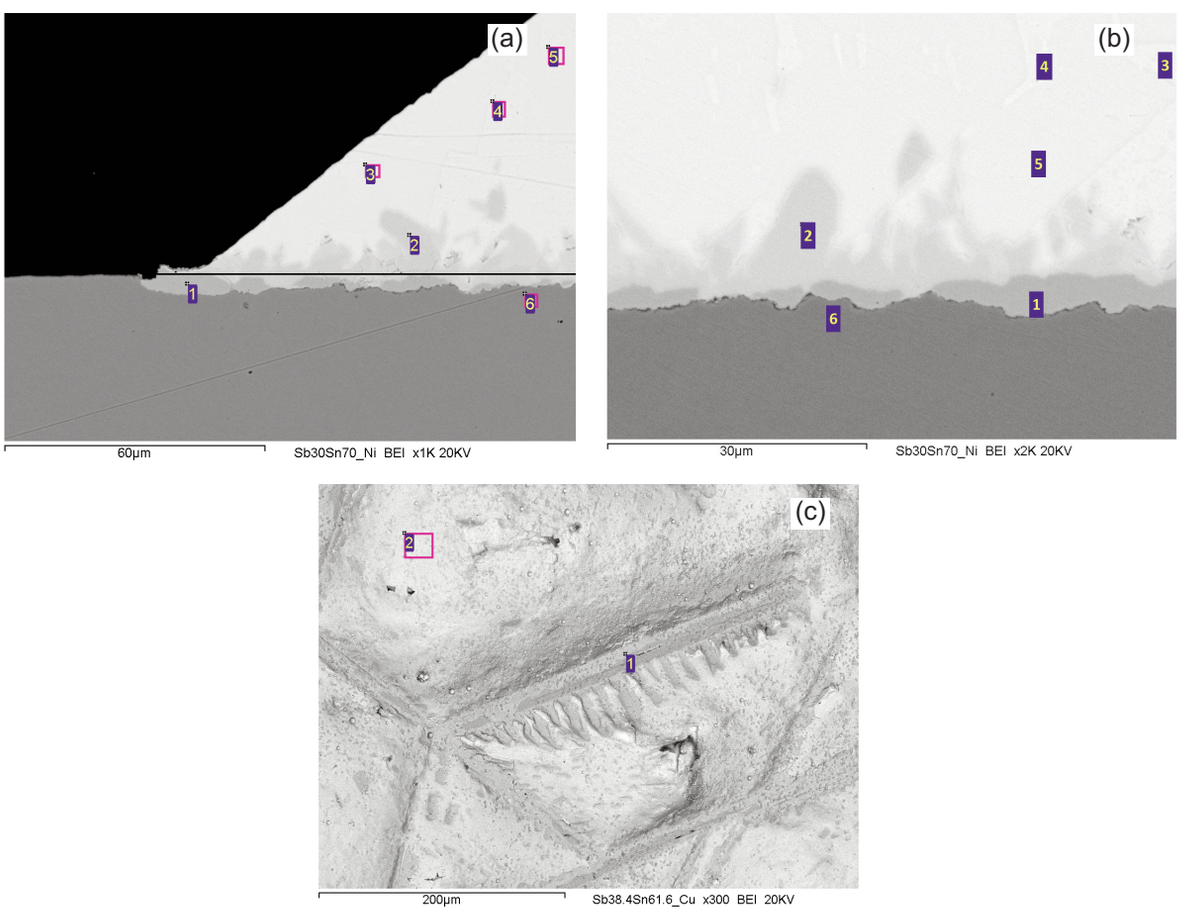

Figure 6. *$Sb_{30}Sn_{70}$ / Ni system. SEM micrograph of a) Cross section of the sessile drop: The formation of one reaction layer at the alloy / substrate interface: 1 – Ni-17.0Sb-10.6Sn (Ni_3Sn based phase); 2 – Ni-37.7Sb-18.5Sn (ζ-based phase near the interface); 3 – 43.1Sb-56.9Sn (SbSn phase); 4 – 9.1Sb-90.9Sn (Sn-rich alloy composition); 5 – 40.7Sb-59.3Sn (close to Sb_2Sn_3 phase); 6 – Ni-substrate. b) Cross section of the solid/liquid interface with one reaction layer (Table 2): 1 – Ni-18.2Sb-9.7Sn (Ni_3Sn based phase); near the interface 2 – Ni-34.1Sb-19.6Sn (ζ-based phase); 3 – 15.6Sb-84.4Sn and 4 – 9.0Sb-91.0Sn (Sn-rich alloy compositions); 5 – 44.0Sb-56.0Sn (SbSn phase). c) Solidified drop border close to Ni-substrate: 1 – Ni-28.9Sb-23.2Sn and 2 – Ni-33.4Sb-18.5Sn (ζ- based phases); 3 – Ni-43.2Sb-52.4Sn (SbSn based phase) and 4 – Ni-39.0Sb-57.1Sn (Sb_2Sn_3 based phase)*

CC BY SA

min at each temperature (Fig. 5; Table 1). During heating up to T = 650 ± 1 K, the initial contact angle was about 127° and it decreased gradually to Θ = 70° measured at the beginning of the first isothermal cycle at 650 K. A further decrease to Θ = 57° was observed after 10 min, followed by a stepwise decrease to Θ = 37° at T = 790 K after 56 min, when the last isothermal cycle was completed (Fig. 5; Table 1).

The solidified $Sb_{30}Sn_{70}$ / Ni sample was metallographically prepared and its cross section was characterised by SEM-EDS analyses. At thr interface one reaction layer with the composition of Ni-17.0Sb-10.7Sn having irregular morphology was observed. The Ni-17.0Sb-10.7Sn is based on the Ni_3Sn phase, which has been found at 773 K in the samples subjected to isothermal solidified without quenching [62]. Near the interface the Ni-34.7Sb-18.5Sn phase was detected (Fig. 6a).

Similar composition described by Ni-35.2Sb-19.3Sn was also found. These phases belong to continuous solid solutions that exist between the two stoichiometric NiSb and Ni_3Sn_2 compositions, and are denominated as ζ - phase [1,61]. Increasing the distance from the interface, the SbSn intermediate compositions of (42.1 ± 1.0)Sb-(57.9 ± 1.0)Sn, 9.1Sb-90.9Sn and 40.6Sb-59.3Sn (Sb_2Sn_3) respectively, were identified (Fig. 6a). An enlarged interface area is shown in Fig. 6b. A very thin irregular interfacial layer (< 6 μm) of Ni-18.2Sb-9.7Sn phase, which is based on Ni_3Sn, and close to the interface, Ni-34.1Sb-19.6Sn solid solution known as ζ - phase (10 μm) were found (Fig. 6b; Table 2). The final operating temperature of 790 K (Table 1) and the formation of ζ - phase are substantiated by the studies reported in [12,60,61]. Near the interface, Sb-56.0Sn (SbSn-phase) was detected, while the two Sn-rich compositions, i.e. 15.6Sb-84.4Sn and 9.0Sb-91.0Sn, were identified as bulk phases (Fig. 6b). The presence of Ni-28.9Sb-23.2Sn and Ni-33.4Sb-18.5Sn alloy compositions (ζ - phases) on the solidified drop border with Ni-substrate and in the vicinity of the interface, respectively, was detected. On the top drop Ni-43.2Sb-52.4Sn (SbSn based phase) and Ni-57.1Sn-39.0Sb (Sb_2Sn_3 based phase) were identified (Fig. 6c), in agreement with [12,61]. Grytsiv et al. [60] reported negligible solubility of Ni in SbSn phase, while significant Ni-solubility was taken into account to reproduce invariant reactions in the temperature range between 523 and 673 K [61]. SEM-EDS data obtained after the wetting tests at 790 K indicated that about 4.4 at % Ni was dissolved in the SbSn phase (Fig. 6c).

3.2.2. $Sb_{38.4}Sn_{61.6}$ / Ni

Due to some problems related to the melting, the alloy sample has been heated under non-isothermal

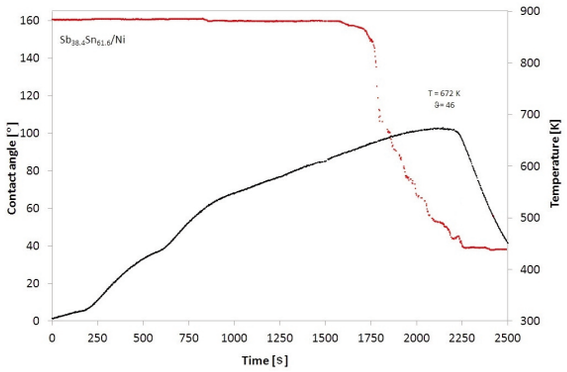

***Figure 7**. Contact angle (◆) and temperature (•) as function of time for the $Sb_{38.4}Sn_{61.6}$ alloy on Ni-substrate*

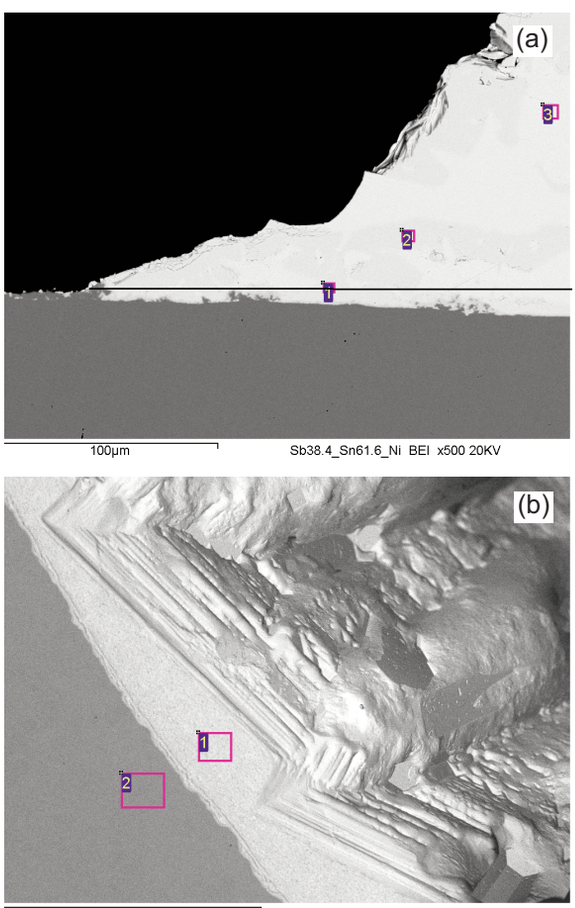

***Figure 8**. $Sb_{38.4}Sn_{61.6}$ / Ni system. SEM micrograph of a) Cross section of the sessile drop: The formation of one reaction layer at the alloy/substrate interface (Table 2): 1 – Ni-46.0Sb-31.7Sn (τ-phase); 2 – Ni-48.0Sb-29.5Sn (τ-phase near the interface); 3 – 44.2Sb-55.8Sn (SbSn phase). b) Solidified drop border close to Ni-substrate: 1 – Ni-30.7Sb-29.6Sn (τ-phase); 2 – Ni-substrate (with a spot of Ni-0.7Sn-0.7Sb)*

CC BY SA

conditions for 30 min. Subsequently, the variations of the contact angle Θ under isothermal conditions at T = 672 K and for time of about 8 ± 1 min were determined (Fig. 7). After the melting of sample, the initial contact angle was about 143°, it decreased monotonically to Θ = 80° at the beginning of the isothermal cycle at T = 672 K and after 8 min, the contact angle Θ = 46° was measured (Fig. 7; Table 1).

The $Sb_{38.4}Sn_{61.6}$ / Ni interface was characterised using SEM and EDS analyses. The interface between the $Sb_{38.4}Sn_{61.6}$ alloy and Ni-substrate remains nearly macroscopically planar. Thin interfacial layer of Ni-46.0Sb-31.7Sn (< 4 μm) and close to it, the phase of similar composition, i.e. Ni-48.0Sb-29.5Sn were detected (Fig. 8a).

The presence of a novel ternary phase, denominated as τ - phase, was found in a non-equilibrium four-phase mixture with binary phases [60]. Therefore, the two aforementioned phases shown in Fig. 8a belong to the Sb-Sn-NiSb-Ni_3Sn_2 system, and they can also be termed as τ- phase. The 44.2Sb-55.8Sn (SbSn phase) was identified in the bulk drop (Fig. 8a). τ- phase, with the composition of Ni-30.7Sb-29.6Sn was also detected on the solidified drop border close to Ni-substrate (Fig. 8b).

4. Conclusions

The sessile drop method has been used to determine the wetting properties of liquid $Sb_{30}Sn_{70}$ and $Sb_{38.4}Sn_{61.6}$ alloys on Cu and Ni-substrates. The two Sb-Sn alloys exhibit a good wetting behaviour characterised by the contact angle values varying between 30 and 45°, respectively, similarly to those measured for Sn-rich solders. After solidification, in the case of Cu-substrates, the microstructural characterisation performed by SEM-EDS analyses indicates the formation of two reaction layers based on the ε-Cu_3Sn and η-Cu_6Sn_5 intermetallic phases, while in the Sb-Sn / Ni systems, Ni_3Sn based interfacial layer was found. For the last mentioned systems, after short time wetting experiments, the presence of τ-phase at the interface was detected. The interfacial layers grown on Cu substrates are thicker with respect to the layers of Ni_3Sn_4 or τ-phase formed on Ni substrates due to faster diffusion rate of copper in liquid Sn. For the systems investigated, an increase in temperature and/or reaction time increases the thickness of interfacial layer and the interfacial reaction kinetics controls the growth of intermetallic compounds. The experimental data on the solid / liquid interactions occurring at the wetting temperature together with the data on subsequent phases formed at the interface can be used to calculate the phase equilibria in the systems tested.

Acknowledgement

The authors would like to thank Dr T. Lanata who performed the wetting experiments during her Post-doc period at CNR-IENI Genoa and Dr D. Li for the alloy preparation during his PhD research stay at DCCI-Genoa University.

References

[1] R. Novakovic, T. Lanata, S. Delsante, G. Borzone, Mater. Chem. Phys., 137 (2012) 458-465.

[2] Yu. Plevachuk, W. Hoyer, I. Kaban, M. Köhler, R. Novakovic, J. of Mater. Sci., 45 (2010) 2051-2056.

[3] R. Novakovic, D. Giuranno, E. Ricci, S. Delsante, D. Li, G. Borzone, Surf. Sci., 605 (2011) 248-255.

[4] M. Abtew, G. Selvaduray, Mater. Sci. Eng. R, 27 (2000) 95-141.

[5] K. Suganuma, Curr. Opin. Solid State Mater. Sci., 5 (2001) 55-64.

[6] V. Sklyarchuk, Yu. Plevachuk, I. Kaban, R. Novakovic, J. Min. Metall. Sect. B-Metall., 48(3) B (2012) 443-448.

[7] T. Gancarz, J. Electro. Mater., 43(12) (2014) 4374-4385.

[8] D. Giuranno, S. Delsante, G. Borzone, R. Novakovic, J. Alloys Compd., 689 (2016) 918-930.

[9] G.Y. Li, B.L. Chen, J.N. Tey, IEEE Transactions on Electronics Packaging Manufacturing, 27(1) (2004) 77-85.

[10] I. Artaki, A. M. Jackson, J. Electron. Mater., 23(8) (1994) 757-764.

[11] http://www.cost.eu/COST_Actions/mpns/MP0602 (final_report-MP0602.pdf, 2012)

[12] G. Borzone et al., in: A. Kroupa (Ed.), COST Action MP0602-Handbook of High-Temperature Lead-free Soldering Systems: Vol.3 - Group Project Reports, COST Office, 2012.

[13] R. Novakovic, Yu. Plevachuk, in: A. Watson (Ed.), COST Action MP0602 - Handbook of High-Temperature Lead-free Soldering Systems: Vol. 2 - Materials Properties, COST Office, 2012.

[14] M. Wachtler, M. Winter, J.O. Besenhard, J. of Power Sources, 105 (2002) 151-160.

[15] A. Trifonova, M. Wachtler, M. Winter, J.O. Besenhard, Ionics, 8(5-6) (2002) 321-328.

[16] H. Guo, H. Zhao, C. Yin, W. Qiu, J. Alloys Compd., 426(1-2) (2006) 277-280.

[17] X.-M. Zheng, L. Huang, Y. Xiao, H. Su, G.-L. Xu, F. Fu, J.-T. Li, S.-G. Sun, Chem. Commun., 48 (2012) 6854-6856.

[18] W. Reinders, Z. Anorg. Chem., 25 (1900) 113-125.

[19] R.S. Williams, Z. Anorg. Chem., 55 (1907) 1-33.

[20] K. Iwasé, N. Aoki, A. Osawa, Scientific Reports of Tohoku Imperial University 20 (1931) 353-368.

[21] K. Schubert, H. Fricke, Z. Metallkd., 44 (1953) 457-461.

[22] B.L. Eyre, J. Inst. Metals, 88(5) (1960) 223-224.

[23] B. Predel, W. Schwermann, J. Inst. Met., 99 (1971) 169-173.

[24] B. Jönsson, J. Ågren, Mater. Sci. Technol., 2 (1986) 913-916.

CC BY SA

[25] W.P. Allen, J.H. Peperezko, Scr. Metall. Mater., 24(11) (1990) 2215-2220.

[26] T.B. Massalski, H. Okamoto, P.R. Subramanian, L. Kacprzak (Eds.), Binary Alloy Phase Diagrams, 2nd Edition, Vols. 1-2, ASM International, Materials Park, OH, 1990, p. 3306.

[27] H. Ohtani, K. Okuda, K. Ishida, J. Phase Equilib., 16(5) (1995) 416-429.

[28] V.P. Vasil'ev, Russ. J. Phys. Chem., 79(1) (2005) 20-28.

[29] A. Kroupa, A. Vizdal, Defect and Diffusion Forum, 263 (2007) 99-104.

[30] S. Chen, C. Chen, W. Gierlotka, A. Zi, P. Chen, H. Wu, J. Electron. Mater., 37(7) (2008) 992-1002.

[31] C. Schmetterer, J. Polt, H. Flandorfer, J. Alloys Compd., 728 (2017) 497-505.

[32] C. Schmetterer, J. Polt, H. Flandorfer, J. Alloys Compd., doi: 10.1016/j.jallcom.2017.11.367

[33] F. Gnecco, E. Ricci, S. Amore, D. Giuranno, G. Borzone, G. Zanicchi, R. Novakovic, Int. J. Adhes. Adhes., 27(5) (2007) 409-416.

[34] S. Amore, E. Ricci, G. Borzone, R. Novakovic, Mat. Sci. Eng. A, 495 (2008) 108-112.

[35] S. Amore, E. Ricci, T. Lanata, R. Novakovic, J. Alloys Compd., 452(1) (2008) 161-166.

[36] C. Leinenbach, F. Valenza, D. Giuranno, H.R. Elsener, S. Jin, R. Novakovic, J. Electron. Mater., 40(7) (2011) 1533-1541.

[37] S. Jin, F. Valenza, R. Novakovic, C. Leinenbach, J. Electron. Mater., 42(6) (2013) 1024-1032.

[38] P. Fima, G. Garzel, A. Sypien, J. Electron. Mater., 43(12) (2014) 4365- 4373.

[39] R.J. Good, J. Adhes. Sci. Technol., 6(12) (2012) 1269-1302.

[40] L. Liggieri, A. Passerone, High Temp. Techn., 7 (1989) 82-86.

[41] P.T. Vianco, D.R. Frear, JOM 45 (1993) 14-19.

[42] N.-C. Lee, White Papers, Indium corporation, 2010, pp.1-8.

[43] R. Gagliano, M.E Fine, JOM, (2001) 53(6) 33-38.

[44] T. Laurila, V. Vuorinen, J.K. Kivilahti, Mat. Sci. Eng. R, 49(1-2) (2005) 1-60.

[45] D. Li, P. Frank, S. Fürtauer, D. Cupid, H. Flandorfer, Intermetallics, 34 (2013) 148-158.

[46] B.-J. Lee, N.M. Hwang., H.M. Lee, Acta Mater., 45(5) (1997) 1867-1874.

[47] Z. Mei, A. Sunwoo, J.W. Morris, Metall. Trans. A, 23A (1992) 857-864.

[48] Y. Guan, N. Moelans, J. Alloys Compd., 635 (2015) 289-299.

[49] Y. Yuan, Y. Guan, D. Li, N. Moelans, J. Alloys Compd., 661 (2016) 282-293.

[50] S.W. Chen, A.R. Zi, W. Gierlotka, C.F. Yang, C.H. Wang, S.K. Lin, C.M. Hsu, Mater. Chem. Phys., 132(2-3) (2012) 703-715.

[51] Y. Yuan, G. Borzone, G. Zanicchi, S. Delsante, J. Alloys Compd., 509 (2011) 1595-1600.

[52] J. Lapsa, B. Onderka, C. Schmetterer, H. Ipser, Y. Yuan, G. Borzone, Thermoch. Acta, 519 (2011) 55-58.

[53] S.W. Chen, A.R. Zi, P.Y. Chen, H.J. Wu, Y.K. Chen, C.H. Wang, Mater. Chem. Phys., 111(1) (2008) 17-19.

[54] C. Lee, C.-Y. Lin, Y.-W. Yen, Intermetallics 15 (2007) 1027-1037.

[55] N. Eustathopoulos, M. Nicholas, B. Drevet, Wettability at high temperatures, 1st ed., Pergamon Materials Series vol. 3, Oxford, 1999.

[56] A. Yassin, R. Castanet, J. Alloys Compd., 314 (2001) 160-166.

[57] A. Yassin, R. Castanet, J. Alloys Compd., 307 (2000) 191-198.

[58] S. Kim, D.C. Johnson, J. Alloys Compd., 392 (2005) 105-111.

[59] C. Schmetterer, H. Flandorfer, K.W. Richter, U. Saeed, M. Kauffman, P. Roussel, H. Ipser, Intermetallics, 15 (2007) 869-884.8

[60] A. Grytsiv, P. Rogl, S. Berger, C. Paul, H. Michor, E. Bauer, G. Hilscher, C. Godart, P. Knoll, M. Musso, W. Lottermoser, A. Saccone, R. Ferro, T. Roisnel, H. Noel, J. Phys. Condens. Mater., 14 (2002) 7071-7090.

[61] A. Kroupa, R. Mishra, D. Rajamohan, H. Flandorfer, A. Watson, H. Ipser, CALPHAD, 45 (2014) 151-166.

[62] D. Gur, M. Bamberger, Acta Mater., 46(14) (1998) 4917-4923.

KVAŠENJE I REAKCIJE NA INTERFEJSU: EKSPERIMENTALNA STUDIJA Sb-Sn-X (X = Cu, Ni) SISTEMA

R.M. Novaković [a*], S. Delsante [a,b], G. Borzone [a,b]

[a] Institut za tehnologiju hemije i energije kondenzovanog stanja materije – Veće za nacionalna istraživanja, (ICMATE-CNR), Đenova, Italija

[b] Odsek za hemiju i industrijsku hemiju, Univerzitet u Đenovi i Istraživačka jedinica Nacionalnog konzorcijuma za nauku o materijalima i tehnologiji (INSTM), Đenova, Italija

Apstrakt

Eksperimentalne studije Cu-Sb-Sn i Ni-Sb-Sn sistema izvode se uz pomoć testova kvašenja, posle kojih slede analize mikrostrukturalne evolucije koja se dešava na interfejsu između tečne legure i supstrata u čvrstom stanju. Eksperimenti kvašenja na $Sb_{30}Sn_{70}$ / (Cu, Ni) i $Sb_{38.4}Sn_{61.6}$ / (Cu, Ni) sistemima izvode se korišćenjem nepomične aparature za kapanje. Prilikom kvašenja, ponašanje dve legure u kontaktu sa Cu-supstratom razlikuje se od ponašanja u kontaktu sa Ni-supstratom. Interfejs Sb-Sn legure / supstrata je opisan SEM-EDS analizom. Uz pomoć odgovarajućih faznih dijagrama proučene su čvrsto-tečne interakcije i faze formirane na interfejsu

Ključne reči: *Eksperiment kvašenja; Sb-Sn legure; Cu i Ni supstrati; interfejs; CALPHAD*

CC BY SA